Case study

Same site, different corrosion phenomena caused by chloride: The effect of the archaeological context on bronzes from Sujialong Cemetery, China

Yijie Hu[a], Yangbo Wei[b], Ling Li[b], Ji Zhang[a], Jianli Chen[a,*]

[a] School of Archaeology and Museology, Peking University, Beijing, China 100871
[b] Hubei Provincial Institute of Cultural Relics and Archaeology, Wuhan, China 430077

ARTICLE INFO

ABSTRACT

The corrosion of archaeological bronzes is a complex process, and different corrosion phenomena can occur even within the same site, while previous studies paid little attention. Different corrosion phenomena can be observed on bronzes unearthed from Sujialong Cemetery, Hubei, China; in particular, some bronzes exhibit severe bronze disease, which is an uncommon phenomenon in Hubei bronzes. Multiple analysis methods were used to identify the corrosion products on the bronzes and to clarify the corrosion mechanisms. The results showed that the different corrosion phenomena were associated with the tomb microenvironment in different areas of the cemetery, which was confirmed by a spatial analysis of the whole cemetery; the outbreak of bronze disease was closely related to the presence of high chloride ion concentrations in the tomb environment and poor preservation conditions after excavation. The different corrosion phenomena are related to the archaeological contexts of the bronzes (especially microenvironments), which have been investigated only superficially in the past.

1. Introduction

The corrosion of archaeological bronzes is a typical phenomenon that is affected by the alloy composition and casting structure of the bronzes as well as the burial environment [1–7], which is related to the archaeological contexts. Analyses of the corrosion products and layer structures of ancient bronzes are of great significance for extracting archaeological and environmental information [8–10], exploring corrosion behaviour [11–15] and preserving historical artefacts [16,17]. Additionally, some scholars have compared different corrosion phenomena among several sites to comprehensively discuss the relevant corrosion factors [4,18–20], while different corrosion phenomena within the same site have not been paid sufficient attention. In fact, different corrosion phenomena must correspond to the difference in some factors in the same site.

Recently, different corrosion phenomena were found on the bronzes from Sujialong Cemetery, which is located on a hillock near the Zhang River in Jingshan, Hubei, China. In 2015-2017, Hubei Provincial Institute of Cultural Relics and Archaeology excavated the tombs in the southern part of Sujialong Cemetery. The tombs are well preserved and have not been robbed, and the funerary objects are mainly bronze vessels. According to the typology research of the artifacts, the era of the Sujialong Cemetery is from Early Spring and Autumn Period to Mid Spring and Autumn Period, corresponding to about 770 B.C to 550 B.C. It is significant to research the history of Zeng State and the relationship between Central Plain and Southern Region of China through the bronzes from Sujialong Cemetery [21].

The bronzes were picked up with their surrounding soil and were not cleaned immediately after excavation. In 2017, the laboratory excavation work was carried out on fairly well-preserved bronzes unearthed from three tombs (M50, M79, M88) of Sujialong Cemetery (Fig 1a, b). However, the light green, powdery copper trihydroxychloride, which is a sign of bronze disease [22], appeared on some bronzes that were excavated from different tombs (such as M26, M85, M102, and M107) and preserved in Jingshan Museum. The conditions in these tombs were obviously unfavourable for the preservation of bronzes (Fig 1c-f). It is noteworthy that various burial conditions may exist within the same cemetery.

Previous studies have found that most of the bronzes excavated from Hubei remain in good condition and rarely exhibit bronze disease [23–31]. However, these previous studies had some shortcomings. First, due to the lack of archaeological context and envi-

* Corresponding author at: School of Archaeology and Museology, Peking University, No 5 Yiheyuan Road, Haidian District, Beijing, China 100871
E-mail addresses: huyijie@pku.edu.cn (Y. Hu), jianli_chen@pku.edu.cn (J. Chen).

Fig. 1. The preservation conditions of several bronzes from Sujialong Cemetery. Good condition: a M79 Dings and Guis; b M88 Fu; With bronze disease: c M85 Fu (pitting corrosion); d M102 Li; e M26 Hu; f M107 Hu.

ronmental information, some researches on the corrosion status of bronzes in museums have only partially focused on the analysis of the bronze alloy properties. Moreover, some scholars analysed soil samples to represent the macroenvironment of the whole cemetery but failed to compare the microenvironments of tombs and the archaeological contexts within the same site; these microenvironments directly affect the corrosion process and the archaeological contexts directly affect the microenvironments.

2. Research aim

This study aims to explain the appearance of different corrosion phenomena and to broaden our understanding of the corro-

sion mechanism of bronzes unearthed from Sujialong Cemetery by analysing the microstructures of the bronzes and the microenvironment of the tombs and considering the complete archaeological contexts (such as the location in the cemetery, the presence of other funerary objects) comprehensively. In addition, this study also provides relevant theoretical support for the conservation of bronzes.

3. Samples and methods

A total of 159 bronzes excavated from 55 tombs were studied in this paper. The corrosion products were sampled without changing the appearance of the objects. To the extent possible, metal matrix

samples were taken from parts of the bronzes that had missing areas. Soil samples were taken from soil attached to the bronzes.

X-ray diffraction (XRD) analysis

XRD was used to identify the phase compositions of the corrosion products. To determine whether the bronze disease exists, the light green corrosion products were analysed preferentially. If there were no light green corrosion products, other color corrosion products (dark green, lime-green, blue, light blue, red, white) would be analysed to determine whether it contained a small amount of basic copper chloride.

XRD was performed in a Rigaku DMax2200 X-ray diffractometer equipped with a Cu Kα radiation source in the 2θ range from 10° to 80° and a tube voltage of 40 KV; current, 100 mA; step, 0.02°; scan speed, 8°/min; divergence slit, 0.5°; anti-scattering slit, 0.5°; and receiving slit, 0.3 mm.

Scanning electron microscopy-energy dispersive spectroscopy (SEM-EDS)

The metal matrix samples were cold mounted with epoxy resin in a certain direction, and were ground and polished to reveal fresh cross-sections. With the advantages of visualization, the compositions of the alloy and corrosion products were analysed with a Hitachi TM3030 scanning electron microscope coupled with a Bruker Quantax 70 energy-dispersive X-ray spectrometer with an accelerating voltage of 15 kV. The test time was based on the stability of the EDS and was usually controlled at 90 s. As the measurement results of the EDS have some errors compared with the true value (Supplementary Material 1), the EDS measurement results of alloy compositions will only be used for qualitative and semi-quantitative analysis.

The sound metal area was chosen for the alloy composition analysis in order to avoid the influence of corrosion products. The error of EDS measured value was no more than 0.7% for elements with larger atomic numbers such as Cu, Sn, Pb. The O content was only used to indicate and determine the degree of corrosion of the sample: if the O content was higher than 1.5%, the corrosion was considered to be serious and the corresponding composition data was not used for semi-quantitative statistical analysis. In addition, since the ancient bronzes are heterogeneous materials due to the element segregation [32,33] and manufacturing process [34] as well as only a few bronzes had the condition to be sampled from different parts, the EDS results of the samples may not completely correspond to the overall alloy composition of the bronzes. Therefore, the box plots were used to show the distribution of measured values, which reflected the overall technical choices of the bronzes from one tomb rather than one specific object.

Optical microscopy analysis

After polishing, the bronze alloy samples with corrosion products were observed using a LEICA DM4500 M metallographic microscope. For each sample, the same area was observed and photographed under bright-field and dark-field conditions.

Soil analysis

pH

A certain amount of soil sample was weighed out, and decarbonized water was added at a ratio of 1:2.5 (g/mL). The mixture was stirred for 5 minutes and left to stand for 30 minutes. The pH of the soil leachate was determined by using a Mettler-Toledo S20-SevenEasy pH meter three times and taken the average value.

Redox potential (Eh)

A certain amount of soil sample was weighed out, and deoxygenized water was added at a ratio of 1:2.5 (g/mL). CS300 electrochemical workstation was used to measure the open-circuit potential of the soil leaching: the platinum electrode was connected to the positive position, and the saturated calomel electrode (SCE) was connected to the negative position. The measure data (E_m) were recorded after the indication stabilized three times and taken the average value $Eh = E_m + E_{SCE}$.

Soluble salt content

Soluble salt contents were measured by ion chromatography after grounding. Anion chromatography was performed using an AS14 separation column with an eluent of 1.0 mmol/L $NaHCO_3$ solution at a flow rate of 1.2 mL/min. Cation chromatography was performed using a CS12A separation column with an eluent of 20 mmol/L methane sulfonic acid solution at a flow rate of 1.2 mL/min. The anion and cation detectors were ASRS-ULTRA automatic electrochemical suppressors with electron capture detectors run in recycle mode with a suppression current of 40 mA. Soluble carbonate and bicarbonate contents were determined by double indicator-titration method with dilute sulphuric acid.

Moisture content

A certain amount of fresh soil samples were weighted and heated 12 hours in an oven in 105 °C and then the water content was measured in percent based on loss of weight after heating.

4. Results and discussion

4.1. Characterization of the corrosion products of the bronzes

According to the XRD results, most of the bronzes unearthed from Sujialong Cemetery are in good condition. Cuprite, malachite, azurite, cerussite and cassiterite are the most common corrosion products of these bronzes. Cuprite and malachite are the common corrosion products of the archaeological bronzes and azurite can also be found commonly on the bronzes excavated from Hubei Province due to the moister, higher-CO_2 burial environmental condition compared with Northern China [23,29]. The presence of cassiterite and cerussite indicates that tin or lead is contained in the corresponding bronze artifacts, while the existence of the alloy elements cannot be ruled out for the samples where cassiterite and cerussite were not detected due to the crystallinity and heterogeneity of the samples.

Atacamite and clinoatacamite, which indicate the occurrence of bronze disease, can also be found on 50 bronzes from 13 tombs (Supplementary Material 2). The corrosion stratigraphy and structure of some bronzes (both well-preserved and bronze disease) can be seen in Supplementary Material 3.

The bronzes with bronze disease were excavated from three areas, as shown in the cemetery plan by the archaeological zoning method (Fig 2): Area I, the south-western corner of the cemetery, with 7 tombs (M68, M82, M84, M85, M86, M87, and M107); Area II, the southern area of the cemetery, with 4 tombs (M97, M102, M104, and M105); and Area III, the north-eastern area of the cemetery, with 2 tombs (M24 and M26).

4.2. Soil analysis results

We conducted the analyses of 19 soil samples collected from bronzes from 17 tombs in Sujialong Cemetery. The results are shown in Table 1.

Most of the soil samples are brown loam, and some are brownish red loam. Their pH values are mostly between 6-7, indicating that these soils are neutral. The range of HCO_3^- in the soil samples
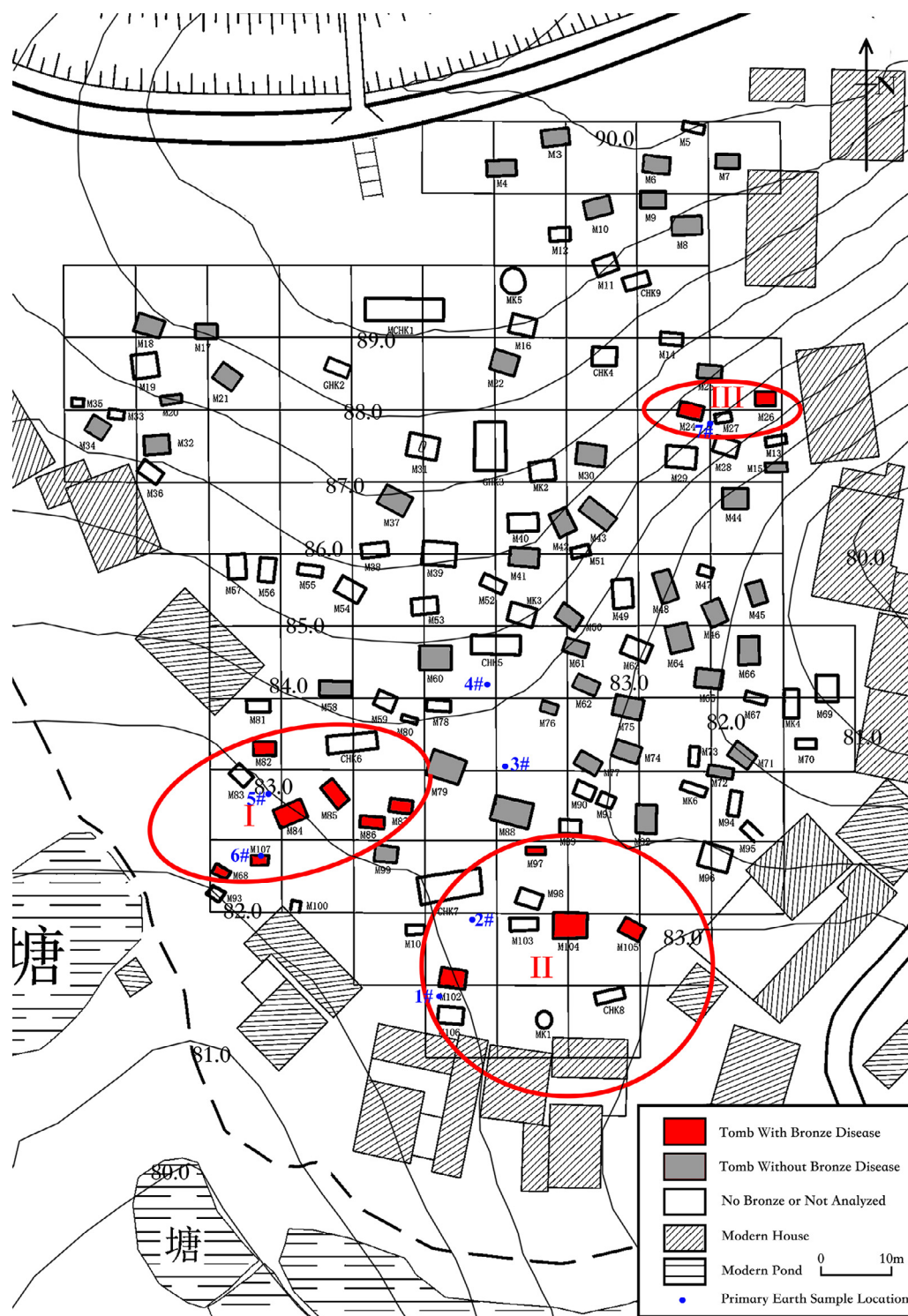
Fig. 2. Sujialong Cemetery plan showing the preservation status of the bronzes.

are from 168.0 to 586.2 mg·kg^{-1}, which is similar to the former results from Hubei [25]. Measuring the chloride ion concentrations in the soil revealed that the Cl^{-} concentrations in the soils of the bronzes with bronze disease could reach 722.8 mg·kg^{-1}, one order of magnitude higher than those in the well-preserved bronzes. This substantial difference in Cl^{-} concentration has a large effect on the stability of corrosion products. The complete results of soil sample analysis can be seen in Supplementary Material 4, 5 and 6.

The redox potential values analysed in the laboratory are in the range of +0.31 V to +0.36 V. However, these are ex situ measurements, and there may be certain deviations between the actual and laboratory values. According to previous studies, mineral soils range in Eh from -0.35 V to +0.75 V [35], and the Eh value of transitional environments (ground water) ranges from +0.2 V to +0.5 V by Schweizer [36]. Since the soil in the tombs was directly back-filled from the local earth, the soil pores, which are channels for

Table 1
The analysis results for soil samples collected inside the bronzes.

Artefact No.	Name	Location	pH	Eh (V)	Cl$^-$ (mg·kg^{-1})	NO$_3^-$ (mg·kg^{-1})	SO$_4^{2-}$ (mg·kg^{-1})	HCO$_3^-$ (mg·kg^{-1})	Bronze Disease
M3:3	Ding	Bottom	6.5	0.34	3.8	2.9	28.2	281.4	No
M8:15	Gui	Bottom	6.4	0.32	2.6	7.8	35.8	325.5	No
M15:4	Ding	Bottom	6.8	0.35	43.0	3.8	22.3	168.0	No
M20:1	Ding	Bottom	6.6	0.33	8.9	1.71	16.9	268.4	No
M25:1	Ding	Bottom	6.6	0.34	14.2	5.2	19.8	334.9	No
M26:2	Hu	Bottom	7.2	0.33	68.1	8.2	11.5	411.4	Yes
M26:3	Ding	Bottom	7.0	0.33	75.0	4.5	36.3	586.2	No
M30:20	Li	Bottom	6.5	0.38	23.8	35.4	64.0	368.8	No
M48:7	Gui	Bottom	6.7	0.33	12.6	2.9	10.9	441.3	No
M72:3	Ding	Bottom	6.5	0.35	7.7	2.2	27.4	215.6	No
M75:2	Ding	Bottom	6.7	0.36	7.3	6.2	28.9	304.6	No
M79:28	Li	Bottom	7.1	0.35	16.1	1.4	9.2	279.6	No
M82:1	Ding	Bottom	6.1	0.35	188.1	2.2	22.4	283.7	Yes
M84:2	Ding	Bottom	6.0	0.36	612.4	3.1	61.8	213.7	Yes
M88:9	Ding	Bottom	7.2	0.34	17.9	2.8	18.5	397.8	No
M88:20	Pan	Bottom	6.6	0.34	17.2	1.0	17.9	326.0	No
M102:11	Li	Bottom	6.1	0.36	124.0	1.1	14.7	426.9	Yes
M105:6	Ding	Bottom	6.2	0.33	439.1	2.4	81.2	295.1	Yes
M107:9	Gui	Bottom	5.9	0.31	722.8	25.6	129.4	432.0	Yes

Table 2
The analysis results of primary earth samples from Sujialong Cemetery.

Sample No	Location of Sample	pH	Eh (V)	Cl$^-$ (mg·kg^{-1})	NO$_3^-$ (mg·kg^{-1})	SO$_4^{2-}$ (mg·kg^{-1})	Moisture Content(%)
1#	M102 Southwest	6.3	0.34	21.0	2.4	83.0	26.0
2#	M102 Northeast	7.1	0.34	30.0	1.5	86.8	18.3
3#	M88 Northwest	7.1	0.38	11.3	4.4	62.1	17.3
4#	M79 Northeast	6.8	0.37	11.9	3.1	54.7	19.9
5#	M84 Northwest	6.4	0.35	35.2	6.9	81.8	22.6
6#	M107 Northwest	5.9	0.34	17.4	5.3	63.0	21.8
7#	M24 Southeast	7.1	0.38	6.9	3.3	54.9	21.9

water and air, were unlikely to disappear. We estimate that the soil potentials in Sujialong Cemetery range from +0.2 V to +0.5 V.

We also analysed 7 primary earth samples from Sujialong Cemetery (Fig 2). The results showed that Cl$^-$ concentrations of the primary earth samples at the site are low, with a maximum of 35.2 mg·kg^{-1}. (Table 2) The Cl$^-$ concentrations in the soil samples collected from the vessels are quite different from the primary earth where bronze disease was found (such as M84, M102, M107). Therefore, the microenvironments of the tombs have an important influence on the bronze corrosion.

4.3. Causes of the different corrosion phenomena

The corrosion of bronzes is a complex process that is often determined by the composition, manufacturing and processing of the bronze alloy (internal factors) and the corrosiveness of the environment (external factors). In discussing the different degrees of corrosion of bronzes excavated from the same cemetery, it is necessary to consider both internal and external factors.

We analysed the alloy compositions of some bronzes from Sujialong Cemetery (Supplementary Material 7). The compositions of the bronze alloy samples exhibit certain variations: The measurement values of tin contents range between 4% and 23%, with an average of 12.6%, and the measurement values of lead contents range between 0 and 18%. The alloy ratio varies depending on the type of vessel, the technical level of vessel production, the status of the vessel owners, the vessel country of origin, and the era from the archaeometry perspective. For example, the tin contents of the bronzes from earlier M79 were lower than that of the later M88's bronzes, indicating that the nobles in the Early Spring and Autumn Period used less tin resources to manufacture the bronzes compared with the Mid Spring and Autumn Period. While in our study, the micro-batteries are formed in the bronzes by the different alloy elements, which influence the corrosion process.

Comparing the measurement values of tin contents of bronzes from different tombs, the bronzes from M79 have the lowest measurements among all the tombs, approximately 8% on average. The measured values of the tin contents of the bronzes from other tombs are between 10% and 15%. It should be noted that the measured values of bronzes with harmful corrosion products, such as M26, M82, M84, M85, M102, and M107, are higher than those of better-preserved bronzes, such as M60 and M79 (Fig 3a). A higher tin content is known to provide better corrosion resistance for copper-tin alloys [28]. Therefore, the tin content is not the main cause of bronze disease in these tombs.

There is a certain deviation for the measurement of lead contents by SEM-EDS, but in this study we only compare the relative amount of lead contents semi-quantitatively. The measurement values of lead contents of the bronze vessels from Sujialong Cemetery fluctuate widely (Fig 3b). Lead is insoluble in copper-tin solid solutions, and its Eh is low; thus, lead corrodes more easily than other elements. However, the bronzes from M107, which have the lowest lead contents among all analysed bronzes, exhibit the most severe bronze disease. Therefore, the alloy composition has limited influence on the different corrosion states of the bronzes unearthed from Sujialong Cemetery.

Moreover, the metallographic structures of the bronzes also have limited influence on corrosion, as evidenced by the fact that equi-axed grains or dendrites can be found regardless of the presence of bronze disease (Supplementary Material 8).

Therefore, in order to explain the different corrosion phenomena among bronzes, environmental factors must be considered. Principal component analysis (PCA) was used to estimate the effect of environmental factors. According to the loading diagram, the contents of soluble salts (Cl$^-$, SO$_4^{2-}$ NO$_3^-$) and acidity properties of the soil samples were represented by the Factor 1, and the Factor 2 corresponded to the acidity, bicarbonate contents and redox properties (Fig 4a). Through dimensionality reduction analy-
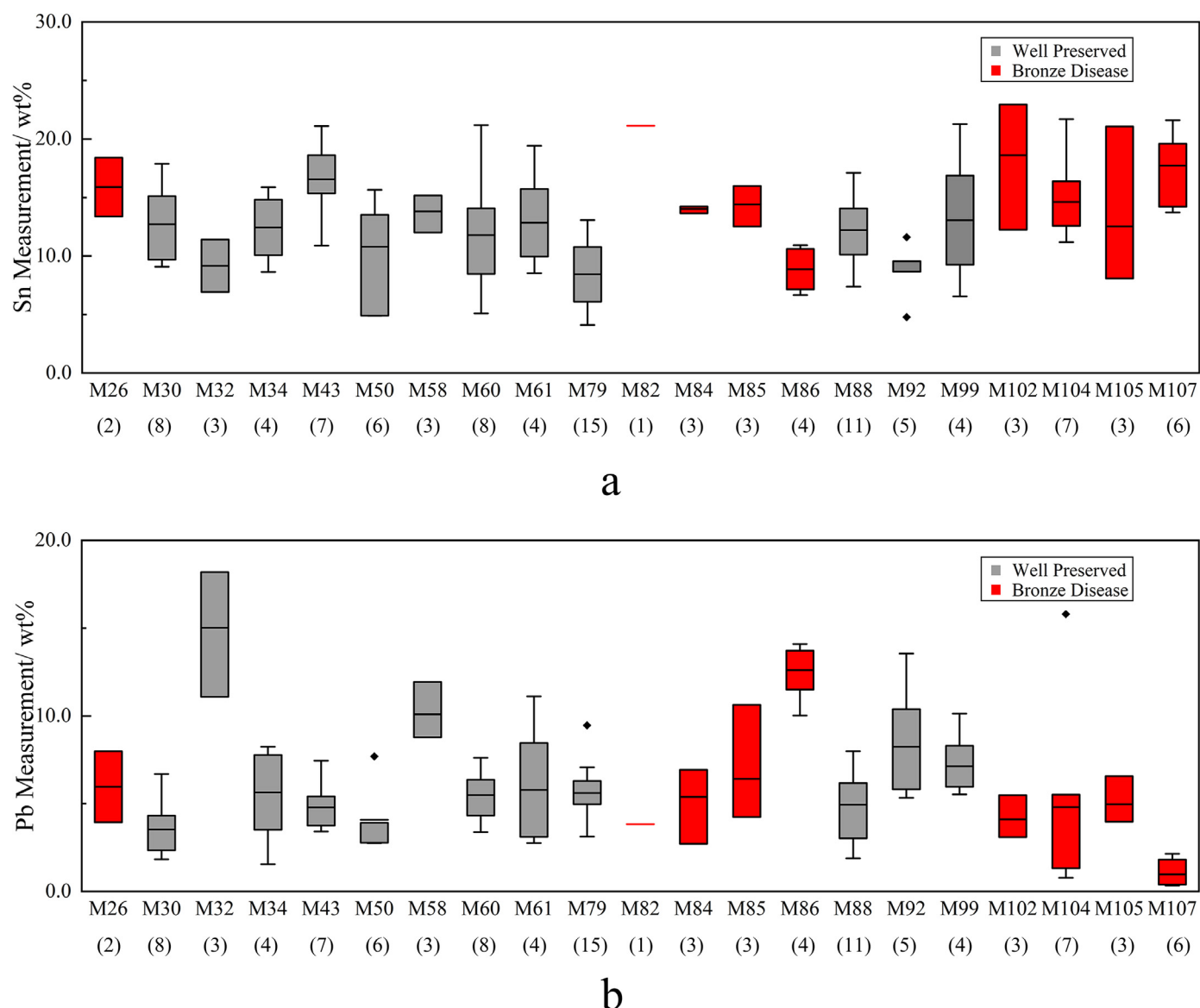
Fig. 3. Boxplot of the tin and lead contents (measurement value) of bronzes from Sujialong Cemetery. a: tin content; b: lead content. The number in brackets represents the sample numbers.

sis (Fig 4b), soil samples without bronze disease are almost gathered in one zone, in addition, the soil sample of the M26 Hu (with bronze disease) is also gathered with the well-preserved bronzes, while the soil samples from Area I (M82, M84 and M107) and II (M102 and M105) are gathered in another zone, corresponding to a lower pH and a higher soluble salt concentration. The soil sample of M30 was also assigned to the samples with bronze disease, corresponding to a higher soluble salt concentration (high nitrate but low chloride concentration makes the bronzes unearthed from M30 without copper trihydroxychloride).

The analysis results of soil samples taken from the bronze vessels show that the soluble salts contents (especially the Cl^-) of soil from the vessels with harmful corrosion are obviously higher than those of soil from the well-preserved vessels. According to the Pourbaix diagram of $Cu-Sn-Cl-H_2O$, when the pH value is 6~7, the Eh value is 0.2 V~0.5 V, and the concentrations of other ions are controlled at 10^{-3} mol/L, cassiterite, cuprite, and tenorite (or malachite and azurite, corresponding to $Cu-Sn-CO_2-H_2O$ system) are in thermodynamically stable phases. If the Cl^- concentration is 355 ppm, at the higher Eh, there is a stable region of copper trihydrox-

ychloride (Fig 5a); if the Cl^- concentration is 35.5 ppm, the region of chlorine-containing corrosion products disappears (Fig 5b). In soils of the bronze vessels unearthed from Sujialong Cemetery that show harmful rust, considering the soil moisture content is approximately 20~25% (Table 2), the Cl^- concentrations are within the range where bronze disease can occur continuously. Therefore, the microenvironments of the different tombs are responsible for the different corrosion phenomena.

Why does the Cl^- concentration vary so much within a small area of the cemetery? We believe that the archaeological context of the site must be considered in this discussion due to the fact that the archaeological context not only provides the information where the bronzes unearthed, but also decides the microenvironment partly. According to the cemetery plan (Fig 2), bronzes that developed copper trihydroxychloride are found in three areas, which suggest that the location chosen for the ancient tombs has influenced the corrosion phenomena. The sloping topography of Sujialong Cemetery is high in the north and low in the south, with an elevation difference of at least 6 metres. The depths of the tombs of high-level nobles (M79, M88) are about 5 meters, and
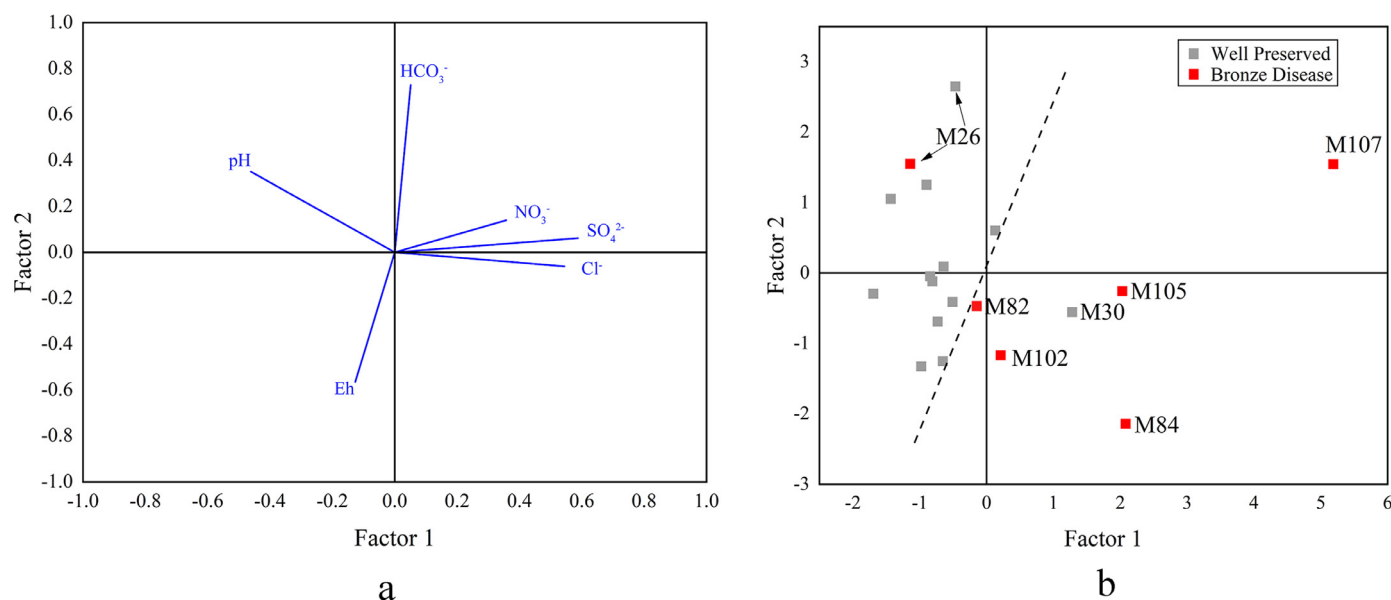
Fig. 4. Principal component analysis of the soil samples from Sujialong Cemetery. a: Loading diagram of variable b: Score diagram of soil samples.
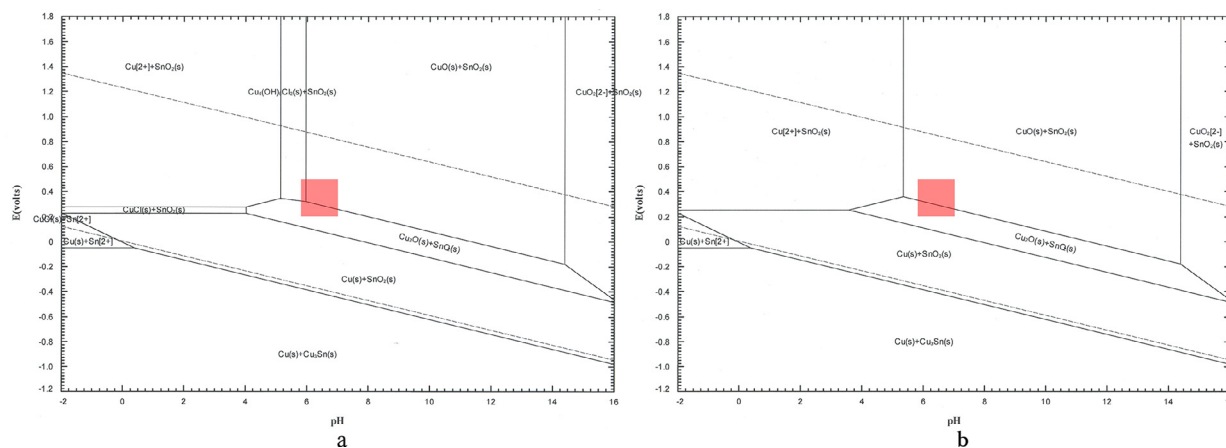

Fig. 5. Pourbaix diagrams of Cu-Sn-Cl-H$_2$O at 25°C [37]. a: pCl=2 (355 ppm), other ion pM=3; b: pCl=3 (35.5 ppm), other ion pM=3. The red zone is the main distribution area of the environmental parameters of Sujialong Cemetery. (For interpretation of the references to colour in this figure legend, the reader is referred to the web version of this article.)

the depths of the medium and small tombs are about 2-3 meters, making the bottom of the tombs where the bronzes located also have altitude differences. However, no tombs were found to be full of water during excavation, indicating that the impact of steady groundwater was limited. The on-site archaeological survey showed that the soil layer in the high-altitude area is thin, and the bedrock is exposed; in this area, the tombs were built directly in rock pits. However, the tombs in the low-altitude area were built in soil pits with poor infiltration, which has caused these tombs to experience alternating drying-wetting conditions due to precipitation. The enrichment of ions through precipitation caused the different bronze corrosion phenomena in the different tombs. Of course, we do not rule out the possibility that the temporary rise of the underground water will enrich the ion concentration. Moreover, it is found that the tombs with bronze disease are concentrated at the edges of the cemetery and close to modern houses. According to the excavators, this area was used by residents in their daily lives, while the area in the centre of the cemetery was less developed. Modern activities may have introduced pollution sources into the soil and altered the ion balance. Thus, the topography of the site and the modern human activities

caused the differences in the burial microenvironment of Sujialong Cemetery.

The results of alloy composition also indicate that the internal alloy of M107 has been preserved in good condition (Supplementary Material 7). We believe that although the soil, which contains a large amount of Cl$^-$, can stabilize trihydroxychloride, the large-scale outbreak of bronze disease may be also related to the post-preservation environment. The bronzes were stored in a plastic storage box directly after being excavated; such storage conditions create a relatively closed environment with high relative humidity, which facilitates the development of bronze disease [38].

The results of PCA implied that the causes of bronze disease unearthed from Area 3 (M24, M26) might not be the same with the ones in the southern area. Through further observation on the bronze Hu unearthed from M26, we found that there are a large number of casting shrinkage holes on the surface (Fig 1e), and the existence of holes provides the necessary conditions for the pitting corrosion [11,12]: the anode reaction occurred in the casting shrinkage cavities, then the pH value decreased and the chloride ions were continuously enriched. When the chloride ion con-

tents have reached the stable level of copper trihydroxychloride, the bronze disease occurs.

5. Conclusion

Different corrosion phenomena can be found on the bronzes from Sujialong Cemetery: Most of the bronzes are well-preserved and in good condition. The corrosion products on the bronzes are mainly cuprite, malachite, azurite, cerussite and cassiterite. However, bronze disease can be found on some of the bronzes. According to the analysis of the microstructure of the bronzes and the microenvironment of the tombs, the presence of copper trihydroxychloride is caused by the high concentration of Cl^- in the tomb soil. The survey of the archaeological contexts revealed that the differential distribution of Cl^- within the same cemetery may be due to the alternating drying-wetting conditions caused by precipitation infiltrating into the different kinds of tombs in the different cemetery areas as well as the pollutants produced by current residents in their everyday lives. In addition, the breakout of bronze disease may also be associated with the post-conservation environment of the bronzes.

Supplementary materials

Supplementary material associated with this article can be found, in the online version, at doi:10.1016/j.culher.2021.08.012.

References

[1] R.F. Tylecote, The Effect of Soil Conditions on the Long-term Corrosion of Buried Tin-bronzes and Copper, J. Archaeolog. Sci. 6 (4) (1979) 345–368, doi:10.1016/0305-4403(79)90018-9.

[2] D.A. Scott, Copper and Bronze in Art: Corrosion, Colorants, Conservation, Getty Publications, Los Angeles California, 2002 Chapter 1.

[3] L. Robbiola, R. Portier, A Global Approach to the Authentication of Ancient Bronzes Based on the Characterization of the Alloy–patina–environment System, J. Cult. Herit. (7) (2006) 1–12, doi:10.1016/j.culher.2005.11.001.

[4] G.M. Ingo, T.D. Caro, C. Riccucci, et al., Large Scale Investigation of Chemical Composition, Structure and Corrosion Mechanism of Bronze Archeological Artefacts from Mediterranean Basin, Appl. Phys. A Mater. Sci. Process. 83 (2006) 515–520, doi:10.1007/s00339-006-3550-z.

[5] F.S. Afonso, M.M. Neto, M.H. Mendonça, et al., Copper Corrosion in Soil: Influence of Chloride Contents, Aeration and Humidity, J. Solid State Electrochem. 13 (2009) 1757–1765, doi:10.1007/s10008-009-0868-4.

[6] O. Oudbashi, Multianalytical study of corrosion in some archaeological copper alloys artifacts, Surf. Interface Anal. 47 (2015) 1133–1147, doi:10.1002/sia.5865.

[7] D.F. Turo, F. Coletti, C.D. Vito, Investigations on Alloy-burial Environment Interaction of Archaeological Bronze Coins, Microchem. J. 157 (2020) 104882, doi:10.1016/j.microc.2020.104882.

[8] G .M. Ingo, T.D. Caro, C. Riccucci, S. Khosroff, Uncommon Corrosion Phenomena of Archaeological Bronze Alloys, Appl. Phys. A Mater. Sci. Process. 83 (2006) 581–588, doi:10.1007/s00339-006-3534-z.

[9] L. Robbiola, P. Moret, T. Lejars, A Case Study of Arthropods Preserved on Archaeological Bronzes - Micro-Archaeological Investigation Helps Reconstructing Past Environments, Archaeometry 53 (6) (2011) 1249–1256, doi:10.1111/j.1475-4754.2011.00607.x.

[10] D.A. Scott, New Insights on the Corrosion of Ancient Bronzes Using X-ray Powder Diffraction: The Importance of Paratacamite, Sampleite, and Connellite, Stud. Conserv. 62 (7) (2017) 410–418, doi:10.1080/00393630.2016.1219466.

[11] V.F. Lucey, Developments Leading to the Present Understanding of the Mechanism of Pitting Corrosion of Copper, Br. Corros. J. 7 (1) (1972) 36–41 http://doi.org/10.1179/000705972798323332.

[12] G. Mankowski, J.P. Duthil, A. Giusti, The Pit Morphology on Copper in Chloride- and Sulphate-containing Solutions, Corros. Sci. 39 (1997) 27–42, doi:10.1016/S0010-938X(96)00100-X.

[13] L. Robbiola, J.M. Blengino, C. Fiaud, Morphology and Mechanisms of Formation of Natural Patinas on Archaeological Cu-Sn Alloys, Corros. Sci. 40 (1998) 2083–2111 http://doi.org/10.1016/S0010-938X(98)00096-1.

[14] C. Xu, J. Wang, Investigation of the Chemical and Electrochemical Behaviour of Mass Transfer at an Archaeological Bronze/Soil Interface, Anti-Corros. Method Mater. 50 (5) (2003) 326–333 http://doi.org/10.1108/00035590310492234.

[15] K. Leyssens, A. Adriaens, C. Degrigny, E. Pantos, Evaluation of Corrosion Potential Measurements as a Means To Monitor the Storage and Stabilization Processes of Archaeological Copper-Based Artifacts, Anal. Chem. 78 (2006) 2794–2801 http://doi.org/10.1021/ac052192s.

[16] R.M. Organ, Aspects of Bronze Patina and Its Treatment, Stud. Conserv. 8 (1) (1963) 1–9, doi:10.1179/sic.1963.002.

[17] M.C. Bernard, S. Joiret, Understanding Corrosion of Ancient Metals for the Conservation of Cultural Heritage, Electrochim. Acta 54 (2009) 5199–5205 http://doi.org/10.1016/j.electacta.2009.01.036.

[18] W. Gerwin, R. Baumhauer, Effect of Soil Parameters on the Corrosion of Archaeological Metal Finds, Geoderma 96 (2000) 63–80 http://doi.org/10.1016/S0016-7061(00)00004-5.

[19] A.G. Nord, E. Mattsson, K. Tronner, Factors Influencing the Long-term Corrosion of Bronze Artefacts in Soil, Prot. Met. 41 (4) (2005) 336–346 http://doi.org/10.1007/s11124-005-0045-9.

[20] O. Oudbashi, A Methodological Approach to Estimate Soil Corrosivity for Archaeological Copper Alloy Artefacts, Herit. Sci. 6 (2018) 2, doi:10.1186/s40494-018-0167-4.

[21] Q. Fang, C. Hu, Q. Xi, Archaeological Achievement of the Sujialong Site, Jingshan, Hubei, Jianghan Archaeol. (6) (2017) 3–9 In Chinese.

[22] D.A. Scott, A Review of Copper Chlorides and Related Salts in Bronze Corrosion and as Painting Pigments, Stud. Conserv. 45 (1) (2000) 39–53, doi:10.1179/sic.2000.45.1.39.

[23] W. Luo, Y. Qin, F. Huang, et al., Study on Corrosion Products of Some Ancient Bronzes Excavated From Hubei Province, Corros. Sci. Prot. Technol. 19 (3) (2007) 157–161 In Chinese.

[24] Z. Huang, C. Pan, W. Ni, et al., Study of Rust-eaten Phenomenon and Mechanism of Bronze Arrows Excavated from Chu Tombs in Middle Yangtze River Region, Sci. Conserv. Archaeol. 20 (4) (2008) 16–25 In Chinese, doi:10.16334/j.cnki.cn31-1652.k.2008.04.004.

[25] P. Jin, Y. Qin, Y. Hu, et al., Analysis of Rusted Residues of Bronze Artifacts from Jiuliandun Tomb No. 1 & 2, Jianghan Archaeol. (1) (2009) 112–119 In Chinese.

[26] W. Luo, R. Jin, Y. Qin, et al., Analysis of the Corrosion Products of the Ancient Bronzes Excavated from Qiaojiayuan Tombs, Appl. Phys. Res. 2 (2) (2010) 156–169 http://doi.org/10.5539/apr.v2n2p156.

[27] Y. Li, Z. Bao, T. Wu, et al., Specific Corrosion Product on Interior Surface of a Bronze Wine Vessel with Loop-handle and its Growth Mechanism, Shang Dynasty, China, Mater. Charact. 68 (2012) 88–93 http://doi.org/10.1016/j.matchar.2012.03.015.

[28] B. Li, X. Jiang, R. Wu, et al., Formation of Black Patina on an Ancient Chinese Bronze Sword of the Warring States Period, Appl. Surf. Sci. 455 (2018) 724–728, doi:10.1016/j.apsusc.2018.06.024.

[29] W. Liu, L. Li, Y. Wei, et al., Study on Corrosion Structure of Bronze Artifacts from Yejiashan Cemetery in Hubei Province, Jianghan Archaeol. (4) (2019) 116–126 In Chinese.

[30] B. Li, X. Jiang, Y. Tu, et al., Inward Growth" Corrosion and its Growth Mechanism in Ancient Chinese Bronzes, MRS Adv. 5 (2020), doi:10.1557/adv.2020.58.

[31] Y. Mu, W. Luo, L. Li, et al., Research on the corrosion product layer of bronzes excavated from Yejiashan Cemetery in Suizhou, Sci. Conserv. Archaeol. 32 (3) (2020) 8–16 In Chinese, doi:10.16334/j.cnki.cn31-1652/k.2020.03.002.

[32] D.A. Scott, in: Metallography and Microstructure of Ancient and Historic Metals, The Getty Conservation Inst., Los Angeles CA, 1994, pp. 25–27.

[33] W.T. Chase, Chinese Bronzes: Casting, Finishing, Patination and Corrosion, in: D.A. Scott, J. Podany, B.B. Consadine (Eds.), Ancient and Historic Metals: Conservation and Scientific Research, The Getty Conservation Inst., Los Angeles CA, 1994, pp. 85–117.

[34] R.J. Gettens, in: The Freer ChineseBronzes, Volume II, Technical Studies, Smithsonian, Washington DC, 1969, pp. 57–120.

[35] L.G.M. Baas Becking, I.R. Kaplan, D. Moore, Limits of the Natural Environment in Terms of pH and Oxidation-Reduction Potentials, J. Geol. 68 (3) (1960) 243–284.

[36] F. Schweizer, Bronze Objects from Lake Sites: From Patina to "Biography", in: D.A. Scott, J. Podany, B.B. Consadine (Eds.), Ancient and Historic Metals: Conservation and Scientific Research, The Getty Conservation Inst., Los Angeles CA, 1994, pp. 33–50.

[37] A. D. Pelton, Calculation and Analysis of E-pH Diagrams Related to the Corrosion of Chinese Bronzes, Report from THERMFACT LTEE, Submitted to: M. Notis, T. Chase, Lehigh University, 2006.

[38] D.A. Scott, Bronze Disease: A Review of Some Chemical Problems and the Role of Relative Humidity, J. Am. Inst. Conserv. 29 (2) (1990) 193–206, doi:10.2307/3179583.